

Implementation of hyperbolic tangent function to estimate size distribution of rock fragmentation by blasting in open pit mines

Hassan Bakhshandeh Amnieh ^{a,*} and Moein Bahadori ^b

^a School of Mining, College of Engineering, University of Tehran, Tehran, Iran

^b Department of Mining Engineering, University of Gonabad, Gonabad, Iran

Article History:

Received: 22 November 2016,

Revised: 09 August 2018,

Accepted: 09 August 2018.

ABSTRACT

Rock fragmentation is one of the desired results of rock blasting. Therefore, controlling and predicting it has direct effects on operational costs of mining. There are different ways to predict the size distribution of fragmented rocks. Mathematical relations have been widely used in these predictions. Among three proposed mathematical relations, one was selected in this study to estimate the size distribution curve of blasting. The accuracy of its estimates was compared to that of the RR (Rosin-Rammler), SveDeFo (The Swedish Detonic Research Foundation), TCM (Two-Component Model), CZM (Crushed Zone Model), and KCO (Kuznetsov – Cunningham - Ouchterlony) relationships. The comparison included assessing the accuracy (Regression, R) and precision (Mean Square Error, MSE) of the best possible fit between the mathematical relations to estimate the cumulative distribution of fragmented rocks that result from rock blasting in open pit mines (Miduk Copper Mine, Sirjan Gol-e-Gohar, and Chadormalu Iron Mines) using image analysis techniques. The results showed that the power hyperbolic tangent function can estimate the size distribution of hard rock fragmentation with more uniformity in fine and coarse-grained sizes (unlike soft and altered rocks with the non-uniform distribution in these regions), more accurately and with higher precision. In addition, unlike the KCO, the absence of a second turning point for the largest block dimensions (X_m) in the proposed function, can guarantee the accuracy of estimations related to any range of inputs. Finally, due to the ability of the proposed relation to accurately estimate the rock fragmentation distribution caused by blasting, the uniformity coefficient required for the relation was provided by a linear combination of the geometric blasting parameters, where $R=0.855$ and $MSE=0.0037$.

Keywords : *blasting, fragmentation, mathematical relations, size distribution*

1. Introduction

An explosion is a very rapid physicochemical phenomenon that releases very high amounts of energy in the form of light, heat, and pressure in a fraction of a second [1-3]. Generally, because of blasting operations, several phenomena occur such as fly rock, ground, and air vibration, back break, fragmentation and pile movement whose prediction and control have an effective role in reducing the operational costs of mining. The main function of each blasting operation is to break a rock into dimensions that the largest fragments would not create any problem for the hauling and loading systems and the finest particles would not cause any disturbance in the mineral processing plant. This range of size distribution minimizes the total cost of production [1, 4]. Due to the inherent heterogeneity of rock masses and the creation of complex fractures during blasting, describing the process of rock breaking that takes place through a blasting mechanism is a complicated task [5]. In any explosion process, the sudden change in the distance among the molecules of explosives from a few angstroms in an unburned explosive to a few millimeters in exploded gaseous products applies shock waves to the rock mass adjacent to the blast hole [1, 6]. The initial energy of the explosion, generally, in production blasting, is so high that a certain range of the blast hole wall will be powdered. Due to the attenuation caused by severe deformations and with an increase in the distance, an area of plastic deformations, which is called the cracked zone, appears around the blast hole outside the powdered zone.

These cracks develop when gaseous products of an explosion leak [1, 4, 7]. Outside the cracked zone, the blasting longitudinal (or compression) waves strike the free surface and are reflected as tensile waves, creating another type of fracture called spalling [1, 4, 7]. Since the speed at which cracks are generated around a blast hole is less than that of the blast waves, the reflected waves create a route that connects two groups of cracks (radial cracks and spalling) and the fragmentation process is completed [7]. In addition, studies conducted by Yang and Rai (2011) showed that increasing the collision chance of the flying blocks in a V-pattern blasting could increase the intensity of fragmentation [8]. Generally, the parameters that affect the results of rock blasting can be divided into two main categories of controllable and uncontrollable parameters. To achieve optimum results in rock blasting, a designer must define the controllable parameters while at the same time taking the uncontrollable parameters into consideration, so that the interaction among all these parameters maximizes the efficiency of blasting operations [9-12]. Accordingly, researchers have tried to include these parameters in mathematical and experimental relations in order to predict rock fragmentation caused by blasting. Such relations could be divided into two general categories: relations that predict the special size of particles (x_{50} , $x_{63.9}$ and x_{80}), and relations that predict size distribution of fragmentation. Larsson (1973) estimated the average size of fragmented rocks taking into account the geometric parameters of explosives, powder factor and the strength properties of the rock mass in an exponential relationship. Although in the relation proposed by Larsson (1973), multiple parameters of rock blasting were taken into consideration, parameters such as the bench height and the length of

* Corresponding author. Tel.: +98-9125230676, E-mail address: hbakhshandeh@ut.ac.ir (H. Bakhshandeh Amineh).

stemming, which play a significant role in the formation of large blocks, were conspicuously ignored [1].

Kuznetsov (1973) proposed a mathematical relation to predict the average size of rock fragments (x_{50}), based on the use of TNT* as the main explosive charge. In this relation, the characteristics of the rock mass were determined according to the Protodyakonov index. The major limitation of this relation was the use of TNT as the main explosive. Moreover, nothing was stated about the uniformity index and fragmentation distribution [13]. Cunningham (1983) extended Kuznetsov's (1973) relation to a variety of explosives, applying the relative energy consumption of a particular explosive compared to TNT [14]. Using the third theory of Bond grinding, Da-Gama (1983) proposed an empirical relation, which could estimate the size of a sieve's span through which 80% of crushed rock passes [15, 16]. In Da-Gama's (1983) relation, the Bond's work index should be determined through operational and experimental methods. In addition, according to Jimeno et al. (1995), direct application of this model in blasting patterns, regardless of the correction factor, can bring about misleading results [1]. Cunningham (1987) modified his previous model [14, 17], in which a blastability index (BI) proposed by Lily (1986) was used to estimate the strength properties of the rock mass instead of Protodyakonov's index [18]. To determine the average size of fragmented rocks, Kuo and Rustan (1993) implemented small-scale explosion tests [19]. In their work, the rock mass impedance determined its strength properties. According to Kihlstrom et al. (1973), patterns with greater S/B (spacing/burden) ratios yield better fragmentation than square patterns. This showed inconsistency with the results obtained by Kuo and Rustan's (1993) relation [20]. Swedish Detonic Research Foundation (SveDeFo) proposed an empirical relation to estimate the average grain size of rock fragmentation by blasting [1]. Sanchidrian et al (2002) calibrated this relation for a variety of rock masses and presented it as an exponential relation [21]. Since the bench height and the stemming length are taken into account in this model, it is expected that the model is more accurate than Larsson's. According to the calculations done using this model, increasing the powder factor, explosive power and S/B ratio reduces the average size of rock fragments [21]. Persson et al (1993) showed that increasing the burden, stemming length and the rock mass constant would increase the average fragmentation size and this was in line with the estimation results obtained through the SveDeFo model [22]. Using a sieve analysis of small-scale blasting fragmentation, Chung and Katsabanis (2000) showed that Cunningham's model (1983) rendered estimations of the uniformity index of fragmentation which were larger than their real values [23]. Therefore, they suggested two relations to determine the uniformity index and the average size of fragmentation. Silva (2006) believes that the size of a sieve span through which 80% of the rock fragments pass (x_{80}) is a function of three factors: Bond work index, RQD and powder factor. He concluded that the Bond work index and RQD directly affected the size of rock fragments while the powder factor had an inverse effect on it. In these relations, there seemed to be a conceptual ambiguity in determining the average grain size. From a statistical point of view, and for normally distributed data, the median and mean values are equal, while in other non-uniform distributions (e.g. lognormal distributions), these two parameters take different values. In this regard, using a dimensional analysis technique, Ouchterlony (2015) showed that misunderstanding the concepts of median and average could cause errors in computing the fragmentation distribution [24].

Several studies focused on the functions that predict the size distribution of rock fragmentation by blasting. Rosin-Rammler's function (1933) was one of the first functions proposed for predicting the fragmentation distribution of fine grain rocks in coal mines [25]. This relation was the basis of many calculations in estimating the size

distribution of fragmented rocks. Using the Griffith theory and taking some assumptions into account, Gilvary (1961) proposed a relation to predict the size distribution of particles in one, two and three dimensions, caused by the generation of a unique crack in solids [26]. To validate the prediction accuracy of the function proposed by Gilvary (1961), Gilvary and Bergstrom (1961) showed the precision of the estimates in predicting the size distribution of broken glass particles (broken under pressure) [27]. Based on Bond index calculations and geometric properties of the blasting pattern, Da-Gama (1970) estimated the energy required to fracture the rock mass and predicted the percentage of fragmented rocks that pass through a specific span size of a sieve [1]. In estimating the size distribution using Da-Gama's (1970) relation, sieve span size with 80% passing rocks has to be known as well as the Bond work index (essentially determined by field tests). Combining the models proposed by Kuznetsov (1973) and Rosin-Rammler (1933), Cunningham (1983) introduced a model (Kuz-Ram model) to estimate the size distribution of fragmented rocks by blasting. This model was the first to calculate the uniformity index (a constant from 0.8 to 2.2) based on the geometric characteristics of the blast pattern [28]. Cunningham (1983) also suggested that for diamond blasting patterns, a value of up to 1.1 should multiply the calculated uniformity index. Da-Gama and Jimeno (1993) proposed an empirical relation for the estimation of the cumulative percentage of particles smaller than a certain size. In this function, parameters such as spacing, burden, average joints spacing and some other constants that represent rock mass strength properties were involved [29]. Grady and Kipp (1985) proposed a binomial exponential function to estimate the distribution of two-dimensional geometric fragmentation [5]. Lu and Latham (1998) considered energy consumption for crushing the rock mass proportional to the area between the size distribution graphs before and after the blasting operation, assuming that the in-situ rock mass is a set of blocks with a given size distribution since it is separated by discontinuities [30]. This model was called "energy-block-transition (EBT)". Kanchibhotla et al. (1999) and Djordjevic (1999) showed that the estimations of the amount of fine-grained crushed rocks obtained through the Kuz-Ram model were lower than the actual values [31, 32]. These researchers believed that estimating the size distribution of the fragmented rock masses with a unique relationship was associated with a high error. Therefore, they proposed a Crushed Zone Model (CZM) and a Two-Component Model (TCM), respectively. These two models were based on a major assumption that a specific cylindrical area around the blast hole was entirely powdered and fractures occurred mainly under tension outside that area. The results of the blast tests performed by Svahn (2002 and 2003) and Moser (2004) showed that the assumption which stated the powdered rocks were limited to a cylindrical zone around the blast hole was not true [33-35]. In the models used by these researchers, the Rosin-Rammler function was applied and the graph was separated into fine and coarse grain sizes at a certain point (characteristic size). Each branch of the graph was developed with its own uniformity. According to Kanchibhotla et al (1999), the position of "characteristic size" depends on the strength of the rock mass and varies from x_{50} for strong rock mass (compressive strength of more than 50 MPa) to x_{90}^{\dagger} for very soft rock mass (compressive strength of less than 10 MPa) [31]. In these models, the uniformity index in the coarse and fine grain ranges is mainly determined by the geometric characteristics of the blasting pattern. However, given that in the two-component model, there are five unknown parameters that must be determined through field tests, this model is more similar to a physical solution compared to the powdered zone model. The studies of Hall and Brenton (2001) showed that although both these models estimated field results to be larger than the results obtained through image analysis technique, the crushed zone

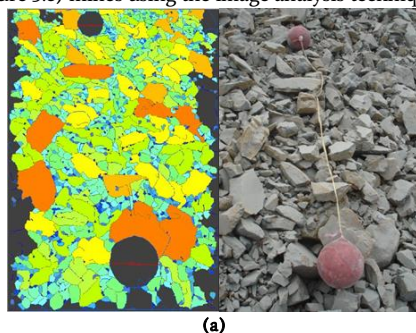
* Trinitrotoluene

† The sieve span size through which 90% of fragmented rocks can pass

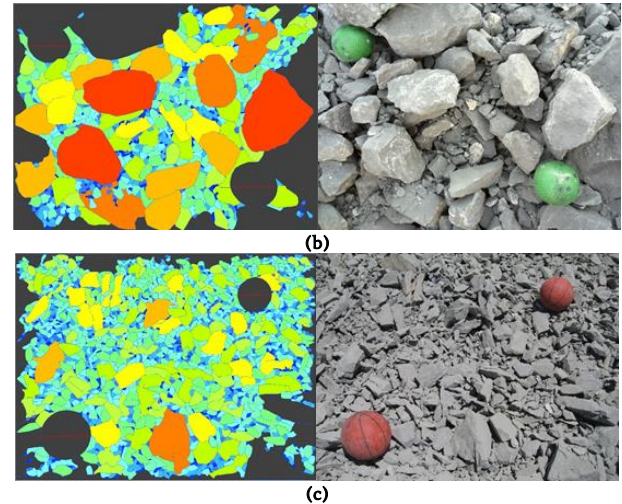
model rendered a better prediction of the fragments' size distribution [36]. The latest function used for predicting the size distribution of rock fragmentation by blasting was proposed by Ouchterlony (2005) and was called the Swebrec function [37]. Calculation of size distribution using the Swebrec function depends on learning the span size of the sieve through which 50% of the fragmented rocks pass (x_{50}), maximum boulder size (X_m), and the curve's fluctuation parameter (b) that is similar to the uniformity index. Ouchterlony (2005) suggested that the x_{50} could be estimated using modified Kuz-Ram [17] or Spathis (2004) [17, 37, 38]. The Studies of Sanchidrián et al. (2014) showed that in comparison with other modified and normalized functions, the Swebrec function estimates the results of fragmentation distribution with a better accuracy [39]. In Sanchidrián et al.'s (2014) reviews, rock fragmentation distribution results of field operations were assessed and compared with the results obtained using Rosin-Rammler model (1933), the Grady and Kipp (1985) two-component exponential function, the log-normal [39], the log-log functions [39], the Gilvary function (1961) and the Ouchterlony function (2005) in the ordinary and normalized modes.

2. Methodology

Assessing methods of rock fragmentation by blasting include sieving, counting the number of large rocks, measuring the amount of explosives used in a secondary blasting, measuring the shovel loading rate, counting the delays encountered in the crushing process, fragmentation index method, experimental models, and probability and image-based methods (e.g. methods of using standard images, scale-based imaging techniques, photographic techniques or manual analysis and image processing techniques). Except sieving that is a direct method, all other methods are classified as indirect methods used to estimate the fragmentation distribution in rock blasting. Image analysis techniques were suggested by Carlsson and Nyberg (1983) and many other researchers that implemented this method to assess the results of rock fragmentation by blasting [8, 28, 40-45]. Due to the speed of implementation, low cost, non-interference in the production process and an acceptable precision, this study adopts an image analysis technique to estimate the size distribution of fragmented rocks caused by blasting. According to Carlsson and Nyberg (1983), the ratio of the largest blocks to the smallest ones in the images should not be greater than 20, and the dimensions of the smallest fragments must be three times larger than the image resolution. Because of a good conformity with the actual mining conditions [45], in this study, the WIPFRAG image analysis software was selected to assess rock fragmentation by blasting. Several images of rock fragmentation from 31 blasting patterns were taken from the surface mines (Miduk copper mine, Gol-E-Gohar Sirjan and Chadormalu iron mines). The images had a high resolution, and were scale-based, and taken simultaneously with the loading process wherever possible. After removing inappropriate cases, 15 to 20 images were selected for each blasting operation to perform the image analysis technique. Figure 1 shows a few examples of the selected images in various rock masses, their scales, and the outputs of the image analysis technique. Figure 2 shows the cumulative passing percent corresponding to the images shown in Figure 1. Figure 3 shows the collections of the measured size distribution of rock fragmentation by blasting in Gol-e-Gohar (Figure 3.a), Chadormalu (Figure 3.b), and Miduk (Figure 3.c) mines using the image analysis technique.



(a)



(c)

Figure 1. An example of analyzed images in assessing rock fragmentation by blasting: (a) The Chadormalu iron mine (Hematite rock mass, the scale size is 20 cm); (b) The Gol-e-Gohar iron mine (Magnetite rock mass, the scale size is 20 cm); and (c) The Midouk copper mine (Phyllic rock mass which consists of quartzite, sericite, and pyrite rocks, the scale size is 23 cm).

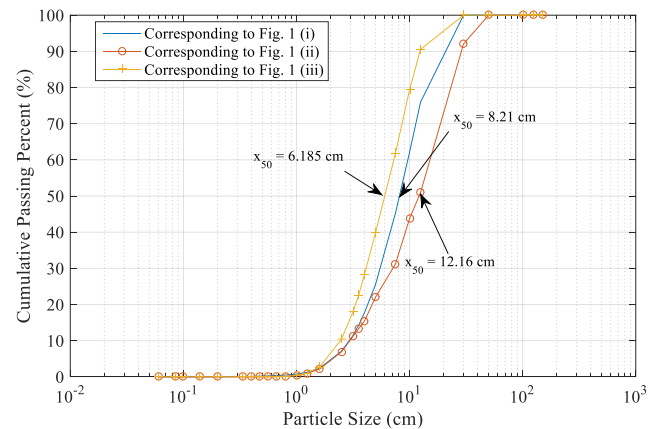
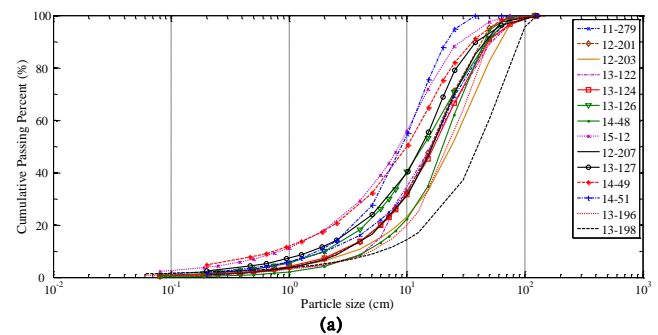
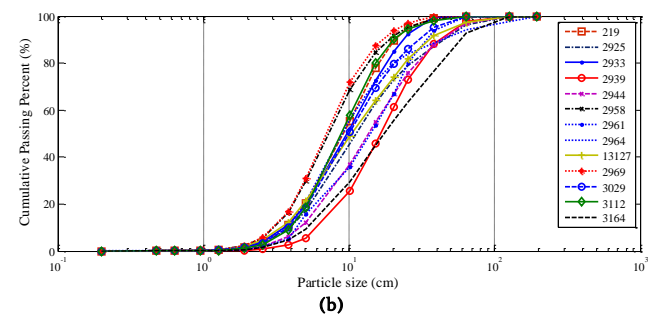


Figure 2. Size distribution of fragmented rocks corresponding to Figure 1.



(a)



(b)

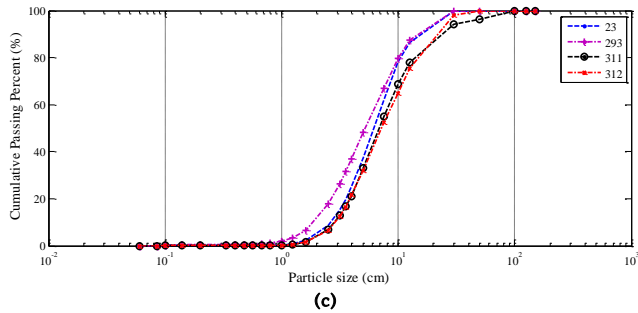


Figure 3. Collections of size distribution data of rock fragmentation by blasting in: (a) Gol-e-Gohar, (b) Chadormalu, (c) Miduk mines.

3. A new mathematical function to predict the distribution of rock fragments

According to Blair (2004), any mathematical function, which increases slowly from zero to one hundred percent, is potentially a predictive function for the cumulative distribution of blast fragmentation [46]. Therefore, several mathematical relationships were examined and two hyperbolic tangent functions and an arctangent function were evaluated for our purpose. The general form of the proposed functions is shown in equations (1) to (3).

$$P_x = \frac{100}{\pi} \times \left[\frac{\pi}{2} + \arctan\left(\frac{x - x_{50}}{\alpha}\right) \right] \tag{1}$$

$$P_x = 50 \times \left[1 + \tanh\left(\frac{x - x_{50}}{\beta}\right) \right] \tag{2}$$

$$P_x = 100 \times \tanh\left(\left(\frac{x}{x_{50}}\right)^\chi \times \delta\right) \tag{3}$$

where, $P(x)$ is the cumulative percent of fragmented rocks passed through a sieve with a span size of x , x_{50} is the average size of the particles, α, β , and χ are the uniformity indexes, and δ is a constant ($\delta = \arcsin(0.5) = 0.5439$). The proposed functions have turning points at $(x_{50}, 50)$ and their skewness changes with an increment in the uniformity index. Figure 4 shows an example of the proposed function behavior with $(x_{50} = 25 \text{ cm})$. As seen, the turning point coincides with the average point $(25, 50)$.

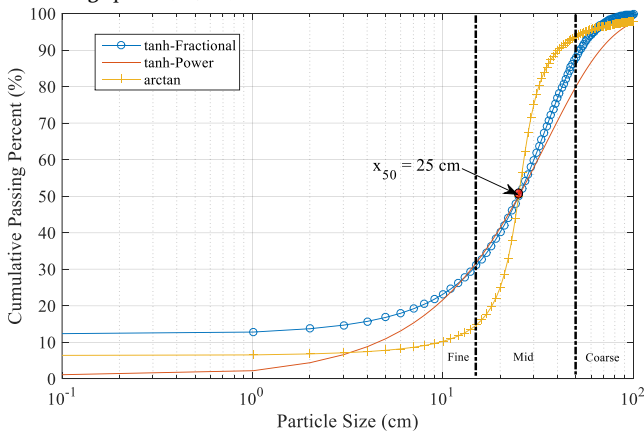


Figure 4. Examples of proposed functions for predicting the distribution of rock fragmentation by blasting.

3.1. Obtaining the predictive functions of the fragments' size distribution

To elaborate the issue, the necessary steps to obtain the predictive relations of the cumulative size distribution of rock fragmentation by blasting are presented in this section, and for brevity only, the Arc-tangent function is described. The behavior of the tangent function is ascending in the range $-\pi/2$ to $\pi/2$, as shown in Figure 5a. As seen, the

effect of the constant coefficient (between 0.25 and 1.25), over which the value of the input x in the tangent function is divided, was studied on the slope and the curvature of the tangent function. This constant coefficient can represent the function of the uniformity coefficient in the proposed function. The general form of the tangent function in this step is explained as Eq. (4)

$$y = \tan\left(\frac{x}{\alpha}\right) \quad \alpha=0.25, 0.50, 0.75, 1.00, 1.25 \tag{4}$$

Figure 5b shows the inverse form of the functions shown in Figure 5a, and as seen in this figure, the inverted functions show a virtual conception of the cumulative distribution of the rock fragments. Eq. (5) shows the inverse form of the tangent function.

$$y = \arctan\left(\frac{x}{\alpha}\right) \quad \alpha=0.25, 0.50, 0.75, 1.00, 1.25 \tag{5}$$

Modifications should be made to convert this form of the Arc-Tangent function to a cumulative size distribution function. First, the input values of the function must be rearranged in such a way that the turning point of the Arc-Tangent function is matched to the x_{50} of the rock fragments. In this step, the form of the tangent function is changed in the form of Eq. (6) and its behavior is shown in Figure 5.c ($x_{50} \neq 0.25$).

$$y = \arctan\left(\frac{x - x_{50}}{\alpha}\right) \quad \alpha=0.25, 0.50, 0.75, 1.00, 1.25 \tag{6}$$

In the next step, it is necessary to make changes so that all the output values of the Arc-Tangent function have positive amounts. Considering the behavior of the Arc-Tangent function, all output values of the Eq. (6) are summed with $\pi/2$ and converted to form Eq. (7) (see Figure 5.d).

$$y = \frac{\pi}{2} + \arctan\left(\frac{x - x_{50}}{\alpha}\right) \quad \alpha=0.25, 0.50, 0.75, 1.00, 1.25 \tag{7}$$

Now, the above relation has two unique features. First, the average value of the output function can be set to any arbitrary x_{50} . Moreover, all of the predicted values of this function have a positive value. However, these positive values do not fit with the expected values in the cumulative distribution of the fragmented material. Therefore, by multiplying the output values of the function in a specific number, the range of the output function should be rescaled in an appropriate range (between 0 and 100). This constant value was chosen as $100/\pi$. Therefore, the final form of the proposed Arc-Tangent function to be used in predicting the cumulative size distribution of the material fragmented by blasting is in the form of Eq. (8).

$$P_x = \frac{100}{\pi} \times \left[\frac{\pi}{2} + \arctan\left(\frac{x - x_{50}}{\alpha}\right) \right] \quad \alpha=0.25, 0.50, 0.75, 1.00, 1.25 \tag{8}$$

Figure 5e shows the corresponding curve and Figure 5.f shows the semi-logarithmic scale form of the above Eq. (8).

3.2. Strengths and weaknesses of the proposed functions and selection of an appropriate function

Comparing the proposed functions shown in Figure 4, one can divide them into three classes of relations related to fine-, medium- and coarse-sized fragments and assess the accuracy and precision of their predictions. In the coarser sizes, the arctangent function behaves more non-uniformly whereas the power hyperbolic tangent function predicts the size distribution with a more uniformity. In the middle section, the arctangent function shows the most uniform distribution and the power hyperbolic tangent function is the most non-uniform. In the fine-grained section, only the results of power hyperbolic tangent function confirm the actual data. The reason is that, as it was expected, the passing percent predicted by power hyperbolic function approaches zero for very small particle sizes. Whereas the two other functions (the fractional hyperbolic tangent function and the arctangent function) do not show such a behavior. Therefore, it can be stated that the power hyperbolic tangent function provides more reasonable predictions of size distribution than the other two functions. For a more comprehensive prediction of size distribution, which covers both coarse size and fine size fragmented rocks, a combination of the power hyperbolic tangent (for $x < x_{50}$) and the fractional hyperbolic tangent functions (for $x > x_{50}$) can be used.

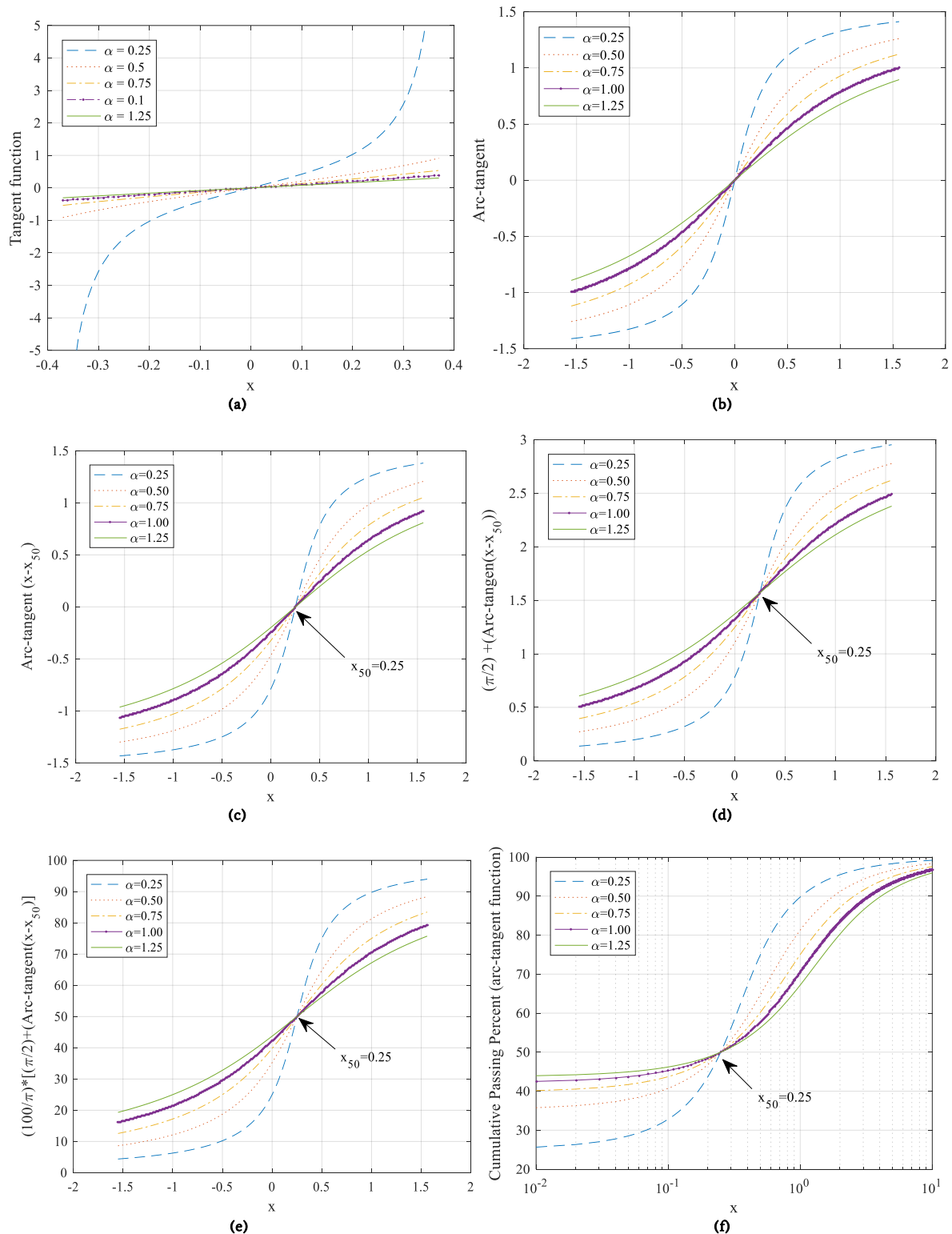


Figure 5. Necessary steps to obtain arctangent function as a size distribution of fragmented rocks.

3.3. Assessment of prediction of rock fragmentation by blasting using the power hyperbolic tangent function and the image analysis technique

To verify the accuracy and precision of the proposed function in predicting the size distribution, the fragmentation data of rock blasting

were measured using the image analysis. Then, the power hyperbolic tangent function was fitted to the measured fragmentation data. For each data set, the best possible fit was performed with maximum correlation and minimum error (using the Solver Add-in in Microsoft Excel), from which R and MSE were obtained. These results were compared with the values obtained by RR, SveDeFo, TCM, CZM, and KCO relations. MSE and R were calculated using Eq. (9) and Eq. (10),

respectively [1].

$$MSE = \frac{1}{m} \sum_{i=1}^m \hat{Y}_i - Y_i^2 \tag{9}$$

$$R = \frac{\left(\sum_{i=1}^m \log \hat{Y}_i \times \log Y_i \right) - \left(\frac{\sum_{i=1}^m \log \hat{Y}_i}{m} \times \frac{\sum_{i=1}^m \log Y_i}{m} \right)}{\sqrt{\left(\sum_{i=1}^m \log \hat{Y}_i^2 - \frac{\left(\sum_{i=1}^m \log \hat{Y}_i \right)^2}{m} \right) \times \left(\sum_{i=1}^m \log Y_i^2 - \frac{\left(\sum_{i=1}^m \log Y_i \right)^2}{m} \right)}} \tag{10}$$

Where, *MSE* is the mean square error (%), *R* is the dimensionless regression, *m* is the total number of the data, \hat{Y}_i and Y_i is the calculated and the measured data (passing percent of fragments) for the i^{th} parameter, respectively.

Table 1. Specification of selected blasting patterns for comparison of the accuracy of mathematical prediction

Mines	Blast No	Pattern Data (m)								Charging		In-situ Data	
		B	S	Hd	Hl	Ch-l	BH	St	Su	Type	PF (kg/m ³)	Density (kg/m ³)	Rock Type
Chadormalu	3112	7.0	8.0	0.251	16.0	9.0	15.0	7.0	2.0	Emulan	0.26	2.7	Metasomatite
	217	4.5	5.5	0.165	11.4	8.0	10.0	3.5	1.5	ANFO	0.23	2.7	Diorite
	2969	4.5	5.2	0.165	11.5	9.0	15.0	5.0	1.0	ANFO	0.23	2.7	Gabro-Diorite
	2961	4.5	5.2	0.165	11.0	9.0	15.0	5.0	1.0	ANFO	0.15	2.7	Metasomatite
	2944	4.5	5.2	0.165	12.6	10.0	15.0	4.5	0.0	ANFO	0.32	2.7	Biotite
	2939	4.5	5.2	0.165	15.0	11.0	15.0	5.0	0.0	ANFO	0.33	2.7	Biotite
	2925	5.2	5.2	0.165	15.0	10.0	15.0	5.0	0.0	ANFO	0.29	2.7	Biotite
	2958	7.0	8.0	0.251	18.4	11.5	15.0	6.5	3.0	ANFO	0.22	2.7	Diorite
	3164	7.0	8.0	0.251	18.0	11.5	15.0	6.5	3.0	ANFO	0.22	2.6	Metasomatite
	3029	7.0	8.0	0.251	15.2	9.0	15.0	7.0	2.0	Emulan	0.26	2.7	Metasomatite
	2933	7.0	8.0	0.251	15.7	9.0	15.0	7.0	2.0	ANFO	0.33	2.7	Metasomatite
	2964	7.5	8.5	0.251	16.0	8.0	15.0	7.0	2.5	Emulan	0.25	2.7	Metasomatite
	219	4.5	5.5	0.165	11.0	6.5	10.0	4.0	1.0	ANFO	0.21	2.7	Diabaz
	Gol-e-Gohar	15-12	5.0	6.0	0.251	11.0	7.6	10.0	3.4	1.0	Emulan	1.47	3.2
14-51		6.5	8.0	0.251	14.0	9.7	13.3	4.3	0.7	Emulan	0.87	3.0	Magnetite
14-49		6.5	8.0	0.251	13.0	8.9	12.3	4.1	0.7	Emulan	0.86	3.4	Magnetite
14-48		5.0	6.0	0.251	13.0	9.0	11.0	4.0	2.0	Emulan	1.6	4.2	Magnetite
13-127		5.0	6.0	0.251	16.9	12.4	13.0	4.5	3.9	Emulan	1.52	3.5	Magnetite
13-126		5.0	6.0	0.251	13.1	8.8	13.0	4.3	0.1	Emulan	1.5	4.1	Magnetite
13-124		5.0	6.0	0.251	13.0	8.8	12.9	4.2	0.1	ANFO	0.93	4.3	Magnetite
13-122		5.0	6.0	0.251	15.0	12.6	14.9	2.4	0.1	Emulan	1.54	3.9	Magnetite
12-207		3.3	3.4	0.152	16.2	13.2	13.8	3.0	2.4	ANFO & Emulan	0.74	3.0	Magnetite
12-203		5.0	6.0	0.251	17.0	12.1	15.8	4.9	1.2	Emulan	1.04	3.2	Magnetite
12-201		5.0	6.0	0.251	17.0	12.5	16.0	4.5	1.0	ANFO & Emulan	0.88	3.1	Magnetite
13-198		3.0	4.0	0.152	14.3	10.3	13.0	4.0	1.3	ANFO & Emulan	0.88	4.3	Magnetite
13-196		3.0	4.0	0.152	15.0	11.0	14.5	4.0	0.5	ANFO & Emulan	0.89	4.3	Magnetite
11-279		3.0	4.0	0.152	17.0	12.2	16.1	4.8	0.9	Emulan	0.87	3.0	Hematite
Midouk	2540-312	6.5	8.0	0.200	17.0	11.0	15.0	6.0	2.0	ANFO	2.1	2.1	Phyllic
	2480-023	5.0	5.5	0.200	17.0	11.0	15.0	6.0	2.0	Emulan	2.4	2.4	Phyllic
	2540-293	6.5	8.0	0.200	17.0	11.0	15.0	6.0	2.0	ANFO	2.25	2.3	Phyllic
	2540-311	6.5	8.0	0.200	18.0	11.0	15.0	7.0	3.0	ANFO	2.2	2.2	Phyllic

The specifications of selected blasting patterns are presented in Table 1. As shown in this table, to overcome the higher strengths of the hard rock masses (frequently iron rocks), the holes were charged with higher powder factors and depending on the water conditions, the ANFO or Emulan was used as the main charge. However, in some unique blasting patterns with the detachment in wet and dry holes, ANFO and Emulan were charged, simultaneously. The hole diameters were 152mm, 165mm, 200mm, and 251mm, and were drilled in burden and spacing in the range of 3m to 7.5m and 3.4m to 8.5m, respectively.

Moreover, considering the adverse orientation and spacing of the joint sets (the average spacing of the joint sets were 2m with the parallel strike to the slope), the powder factor used in blasting patterns of Gol-e-Gohar Iron mine was higher than the other two mines.

Since the goal of this study was to compare the results of the best possible fit of mathematical relations to the measured fragmentation data, the effect of in-situ parameters such as rock strength properties and discontinuities were neglected.

Table 2 presents the results of the best possible fit of the RR, SveDeFo, TCM, CZM, KCO, and Tanh-power relations to the fragmentation data obtained from image analysis. Cases with better compliance are highlighted in Table 2. As can be seen, compared to other mathematical relations, the KCO and Tanh-power relations show better fit (lower MSE and higher R) in most cases. In addition, for the

purpose of carrying out a general comparison, the average values of MSE and R for different cases for each mathematical relation were calculated. These comparisons show that the Tanh-power and the TCM relations have the best and worst average values, respectively. As shown in Table 2, for the best possible fit of the mathematical relations to the measured data, high levels of accuracy can be obtained ($R=1$ in many cases). However, in case of hard rocks, the proposed function often shows better agreement with the data in comparison with the other mathematical relations. On the other hand, for the altered and soft rock masses with lower uniformity in the coarse and fine-grained fragments, the KCO relation shows better fit in most cases. Cases with a better agreement (the higher *R* and the lower *MSE*) are highlighted in Table 2.

3.4. Qualitative and quantitative analysis of results

As stated in Table 2, the KCO function shows better agreement in predicting the size distribution of fragmented rocks with non-uniformity in coarse and fine sizes. This occurs due to the mathematical behavior of the functions. Unlike all other types, the KCO function has two turning points in the average (X_{50}) and maximum (X_m) sizes. The general form of the KCO relation is shown in Eq. (11) [37].

$$P_x = \frac{1}{1 + \left[\frac{\ln\left(\frac{X_m}{x}\right)}{\ln\left(\frac{X_m}{x_{50}}\right)} \right]^b} \quad (11)$$

$$b = 2 \ln 2 \ln \left(\frac{X_m}{x_{50}} \right)^n \quad (12)$$

$$n = \left[2.2 - 14 \frac{B}{H_d} \right] \times \left[1 - \frac{E_p}{B} \right] + \left[\left(1 + \frac{S/B - 1}{2} \right)^{0.5} \right] \times \left[\frac{L}{H} \right] \quad (13)$$

$$x_{50} = A \left(\frac{V}{PF} \right)^{0.8} Q_e^{\frac{1}{2}} \left(\frac{115}{S_{ANFO}} \right)^{19} \quad (14)$$

$$A = 0.06 \times RMD + RDI + HF \quad (15)$$

Table 2. The comparison of the accuracy and precision of mathematical relations predicting the rock fragmentation distribution from surface blasting obtained from image analysis. This is evaluated by obtaining the higher R and the lower MSE

Mine	Blast No.	x ₅₀ (mm)	RR		SveDeFo		TCM		CZM		CZM		Tanh-power		KCO		
			R	MSE	R	MSE	R	MSE	R	MSE	R	MSE	R	MSE	R	MSE	
Chadormalu	3112	98	0.9991	4.35	0.9967	22.30	0.9896	64.40	0.9999	0.33	0.9996	1.83	0.9999	0.48	1.0000	0.10	
	217	97	0.9996	2.15	0.9981	14.91	0.9919	52.23	1.0000	0.10	0.9997	1.60	0.9999	0.53	0.9998	0.91	
	2969	77	0.9988	5.86	0.9968	21.59	0.9890	65.52	1.0000	0.11	0.9997	1.61	0.9999	0.22	0.9999	0.40	
	2961	107	0.9950	21.89	0.9947	22.34	0.9900	47.15	0.9992	2.64	0.9989	4.14	0.9992	2.65	0.9986	6.11	
	2944	80	0.9986	6.68	0.9976	16.02	0.9918	52.13	1.0000	0.13	0.9997	1.63	1.0000	0.20	0.9999	0.48	
	2939	147	0.9985	6.11	0.9985	6.42	0.9956	25.16	0.9999	0.46	0.9996	1.96	0.9998	0.58	0.9998	0.92	
	2925	103	0.9995	2.51	0.9989	9.31	0.9938	40.63	1.0000	0.05	0.9997	1.55	0.9999	0.52	0.9997	1.22	
	2958	150	0.9992	3.03	0.9991	5.42	0.9948	28.86	0.9999	0.28	0.9996	1.78	0.9992	2.83	0.9987	4.47	
	3164	191	0.9981	6.88	0.9976	7.84	0.9970	15.35	0.9998	0.57	0.9995	2.07	0.9995	1.63	0.9993	2.49	
	3029	119	0.9984	6.99	0.9983	9.21	0.9942	35.35	0.9999	0.22	0.9996	1.72	0.9998	0.67	0.9998	0.98	
	2933	173	0.9992	3.40	0.9983	9.42	0.9929	37.27	0.9997	0.93	0.9994	2.43	0.9998	0.68	0.9999	0.37	
	2964	120	0.9982	7.60	0.9980	7.75	0.9964	21.79	1.0000	0.13	0.9997	1.63	0.9997	1.29	0.9996	1.59	
	219	128	0.9970	11.73	0.9970	11.78	0.9950	27.13	0.9997	1.01	0.9994	2.51	0.9997	1.14	0.9995	2.03	
	Gol-e-Gohar	15-12	85	0.9993	1.87	0.9970	25.44	0.9995	2.69	0.9995	1.35	0.9992	2.85	0.9999	0.22	0.9999	0.18
		14-51	92	0.9997	1.53	0.9998	2.21	0.9981	7.75	0.9997	1.09	0.9994	2.59	1.0000	0.16	1.0000	0.10
14-49		100	0.9992	2.42	0.9963	52.09	0.9994	10.43	0.9993	1.99	0.9990	3.49	0.9999	0.34	0.9999	0.14	
14-48		206	0.9996	1.45	0.9994	1.92	0.9994	1.88	0.9997	1.10	0.9994	2.60	0.9999	0.32	0.9999	0.24	
13-127		134	0.9990	3.01	0.9987	18.46	0.9992	2.86	0.9994	1.73	0.9991	3.23	0.9997	0.96	0.9997	0.83	
13-126		138	0.9999	0.20	0.9965	16.78	0.9999	0.26	1.0000	0.16	0.9997	1.66	0.9999	0.17	0.9992	3.01	
13-124		173	0.9999	0.44	0.9989	7.07	0.9999	0.23	0.9999	0.25	0.9996	1.75	1.0000	0.15	0.9984	5.46	
13-122		161	0.9999	0.17	0.9975	13.50	0.9999	0.14	0.9999	0.16	0.9996	1.66	1.0000	0.04	0.9981	4.96	
12-207		165	0.9998	0.75	0.9996	3.69	0.9999	0.33	0.9998	0.64	0.9995	2.14	0.9999	0.28	0.9981	7.55	
12-203		239	0.9993	2.05	0.9987	7.27	0.9996	1.32	0.9994	1.94	0.9991	3.44	0.9998	0.40	0.9961	11.16	
12-201		160	0.9999	0.55	0.9996	2.64	0.9999	0.21	0.9999	0.26	0.9996	1.76	1.0000	0.05	0.9980	6.88	
13-198		409	0.9977	7.79	0.9983	9.41	0.9980	6.34	0.9997	0.58	0.9994	2.08	0.9995	1.37	0.9935	20.69	
13-196		234	0.9994	2.33	0.9995	2.34	0.9994	1.91	0.9999	0.26	0.9996	1.76	0.9998	0.71	0.9980	8.11	
11-279		166	0.9994	2.19	0.9983	11.76	0.9996	1.68	0.9995	1.73	0.9992	3.23	0.9997	0.81	0.9969	10.92	
Midouk		312	72	0.9987	4.85	0.9968	13.22	0.9901	40.64	0.9997	1.14	0.9994	2.64	0.9997	1.18	0.9997	1.05
	23	63	0.9995	2.05	0.9964	17.34	0.9888	50.46	0.9999	0.22	0.9996	1.72	0.9999	0.34	0.9999	0.22	
	293	52	0.9992	3.17	0.9989	5.47	0.9946	27.20	0.9999	0.23	0.9996	1.73	0.9998	0.77	0.9998	0.58	
	311	69	0.9987	4.85	0.9968	13.22	0.9901	40.64	0.9997	1.14	0.9994	2.64	0.9997	1.18	0.9997	1.05	
Average			0.9989	4.22	0.9979	12.52	0.9957	22.90	0.9998	0.74	0.9995	2.24	0.9998	0.74	0.9990	3.39	

where, $P(x)$ is the cumulative passing percent of fragmented rocks from a sieve with the span size of x , x_{50} is the average size, X_m is the maximum block size, b is the fluctuation parameter, n is the uniformity index (0.8 to 2.2), B is the burden (m), H_d is the hole diameter (mm), L is the total length of explosive in the blast hole (m), H is the hole depth

(m), E_p is the actual deviation of the hole (m), S is the spacing (m), A is the rock factor, S_{ANFO} is the relative weight strength of the used explosive to ANFO[‡] (%), Q_e is the charge weight in each blast hole (kg), PF is the powder factor (kg/m³), V is the total volume of pattern, RMD is the rock mass description[§], RDI is the rock density influence^{**}, and HF is the

‡ Ammonium Nitrate Fuel Oil

§ RMD = 10 (for powdery/friable rocks), 50 (massive rocks), JF (for vertical joints)

JF (Joint Factor) = JPS (Joint Plane Spacing) + JPA (Joint Plane Angle)
 JPS = 10 (average joint spacing < 0.1 m), 20 (average joint spacing = 0.1

m), 50 (oversize)

JPA = 20 (dip out of face), 30 (strike perpendicular to face), 40 (dip into face)

** RDI = [0.025 * rock mass density (kg/m³)] - 50

hardness factor^{††} [37].

Figure 6.a shows an example of a cumulative distribution predicted by the KCO relation for the maximum block size of ($X_m=1$ m), with the average sizes of 15 cm and 25 cm and the fluctuation parameter of $b=3$. In addition, based on the KCO prediction, for the same values of fluctuation parameter and the average size ($b=3$ and $x_{50}=25$ cm, respectively), the effect of changing the largest block size on the distribution of fragments is shown in Figure 6.b. It should be noted that in calculating the fluctuation parameter b , the maximum block size is also effective but its effect is negligible.

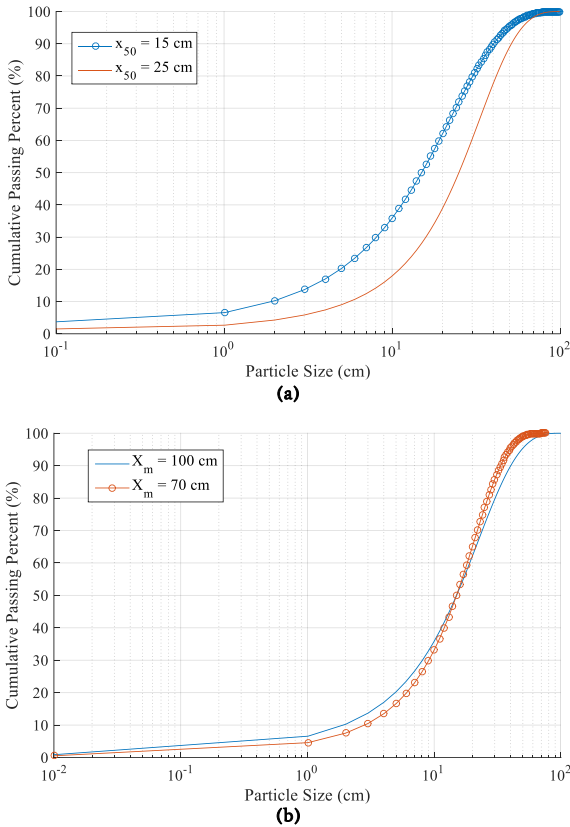


Figure 6. Effect of a. average size (x_{50}) and b. maximum size (X_m) changes on the cumulative distribution predicted by the KCO relation.

Another point is that, based on the Ouchterlony's (2005) recommendation, X_m must be determined as the minimum value for one of these three parameters: minimum in-situ block size, spacing, and burden. But it should be noted that although the maximum value as a second turning point increases the degree of freedom and provides a better adaptation of the KCO function to the data, for the conditions where the input value of (x) is greater than the expected X_m (for any reason), the curve behavior will be different. Figure 7 shows an example of a situation where the distribution of fragmentation must be predicted in the case of $x_{50}=15$ cm, $b=3$, and $X_m=100$ cm (the maximum expected block size) in which a block with the size of 200 cm is produced. This is a failure of the KCO function. It can be stated that if the expected X_m is smaller than the X_m observed in the image, the cumulative percentage is predicted (by the KCO relation) to be greater than 100%. Therefore, the use of maximum size can sometimes lead to errors in estimating the fragments distribution of rock blasting through the KCO relation.

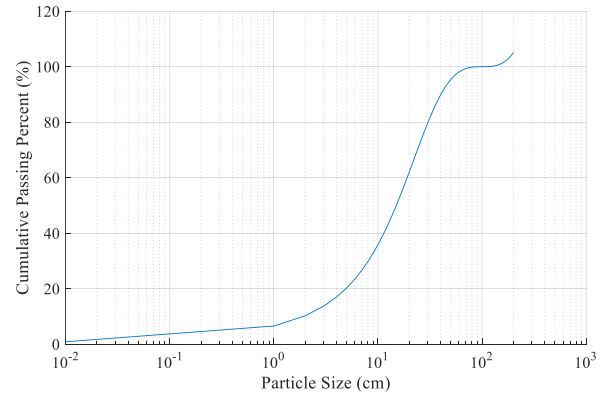


Figure 7. Unexpected behavior of the KCO relation in predicting the cumulative passing percent of inputs greater than X_m .

3.5. Determining uniformity index (χ) and average size (x_{50}) for the proposed function

As shown in Eq. (3), predicting the cumulative distribution of rock fragmentation by blasting with this function, requires determining the uniformity index (χ) and the average size (x_{50}). To determine the uniformity index in Eq. (3), statistical analyses were performed on the blasting input data (including the pattern geometry and the powder factor). It was concluded that each set of the pattern geometry and the powder factor had a meaningful effect on χ . Figure 8.a shows the relation between the stemming length and the best values obtained for χ and Figure 8.b represents the relation between the best values obtained for χ and the powder factor.

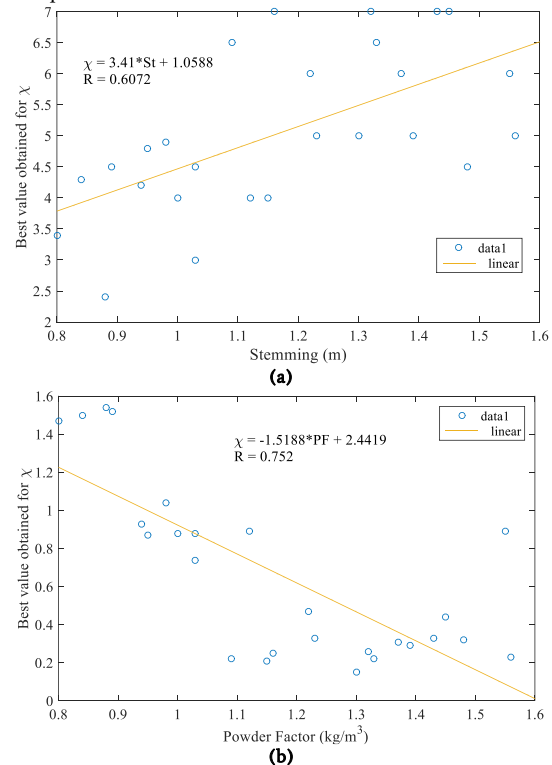


Figure 8. The relation between the best values obtained for χ to a. the stemming length and b. the powder factor.

To obtain a meaningful mathematical relation that can predict χ , all the input data were imported to the trial version of the DataFit software

^{††} HF = E/3 (if E < 50 GPa), $\sigma_c/5$ (if E > 50 GPa)

E = elastic module (GPa), σ_c = unconfined compressive strength (MPa)

V. 9. The software processed the results taking into account a list of many different relations including linear, polynomial, exponential, power-law as well as their combinations. For each relation, the software determined the constant MSE and R values. Afterward, the linear algebraic function with the best regression and the lowest mean square error was selected. This relation is shown in Eq. (16).

$$\chi = a_1 \times B + a_2 \times S + a_3 \times H_d + a_4 \times Chl + a_5 \times BH + a_6 \times St + a_7 \times Su + a_8 \times PF + a_9 \quad (16)$$

where, B is the burden (m), S is the spacing (m), H_d is the hole diameter (mm), Chl is the charge length in the hole (m), BH is the bench height (m), St is the stemming length (m), Su is the sub-drilling (m), PF is the powder factor (kg/m^3), and a_1 to a_9 are the constants determined to be 0.2327, -0.1343, $-3.73e-3$, $-2.27e-2$, $3.72e-2$, $5.15e-2$, $-3.25e-3$, $5.72e-3$, and 1.004, respectively. Comparing the best obtained values of χ (presented in Table 1), with the values calculated by Eq. (16), it is obvious that the proposed Eq. (16) can predict the uniformity indexes for the power hyperbolic tangent function, with the accuracy of $R=0.855$ and the precision of $MSE=0.0037$ (both are dimensionless). In Figure 9, it is shown that χ values obtained from the best fit to the measured data are reasonably consistent with the χ values, which are calculated using Eq. (16).

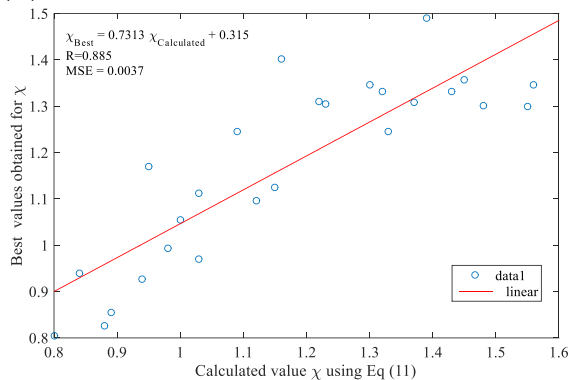


Figure 9. Accuracy and precision of prediction about the best fit values of χ using Eq. (16).

It is also suggested that the average size of fragments (x_{50}) required in the proposed function could be calculated using Eq. (14). Examples of power hyperbolic tangent function with the average size of 25 cm and the uniformity indexes of 0.5, 0.75, and 1 are shown in Figure 10.

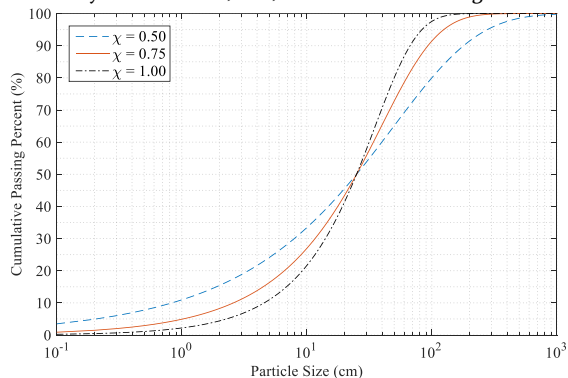


Figure 10. Effect of uniformity index increments on the behavior of power tangent hyperbolic function.

4. Conclusion

The main aim of any blasting operation is to turn rocks into a range of fragments where the fine particles do not interfere with the mineral processing operations and the larger blocks do not cause difficulties in the hauling and loading systems. Therefore, the methods that can use the geometric and structural conditions of the blasting patterns and accurately predict the result of rock fragmentation may considerably reduce the costs of drilling and blasting operation and subsequently reduce the production costs. In order to predict the size distribution of

fragmented rocks obtained by blasting, three mathematical relations were suggested and the power hyperbolic tangent function was selected. Since the latest and the most comprehensive function ever presented to estimate the cumulative distribution of rock fragmentation by blasting is the KCO function, the results of the image analysis in the fragmentation of surface rock blasting were collected for different rock masses, a variety of blast patterns and different used explosives in some open pit mines (Miduk copper mine, Gol-e-Gohar and Chadormalu iron mines). The accuracies of the proposed function was compared with the KCO function in the best possible fit. Unlike other experimental functions, KCO has two different turning points in average and maximum sizes. Therefore, the estimation of a passing percent of the input sizes larger than the expected maximum size could impair the predictions. The proposed function, on the other hand, has only one turning point in the average size with the ability to change the uniformity index and slowly reaching the maximum value. Compared with KCO and the previously proposed functions (high regression and less mean square error), the proposed function in this study has a better agreement in estimating the cumulative distribution of the fragmented hard rocks for the best possible fit. Although for soft and altered rocks the conditions are different, predictions made by the proposed function show acceptable results. In order to determine the required uniformity index based on the acceptable accuracy and precision of the proposed function, a linear polynomial regression relation of blasting pattern was provided with a regression and MSE of 0.885 and 0.0037, respectively. It is also recommended that the modified Kuz-Ram model (1983) can be used for the required average value of the function.

Acknowledgments

The authors would like to express their deepest gratitude and appreciation to engineers Asadollah Khajehzadeh, and Seyed Majid Mousavi (Miduk copper mine), Masoud Asgari and Khabat Amiri (Gol-e-Gohar Sirjan iron mine), Amin Amrollahi Biucki (Chadormalu iron mine), Abolfazl Mir-Hosseini (Bisotun Kavir Company) and Mohammad Reza Dehghan Niri (Padra Madan Iranian Company) who provided us with the ability to have access to, collect and record the fragmentation data.

REFERENCES

- [1] Jimeno CL, Jimeno EL, Carcedo FJA. Drilling and Blasting of Rocks. Rotterdam, Netherlands: AA Balkema; 1995.
- [2] Cooper PW. Explosives Engineering. Canada: Wiley-VCH, Inc.; 1997.
- [3] Hustrulid W. Blasting Principles for Open Pit Mining: AA Balkema, Rotterdam, Netherlands; 1999.
- [4] Hustrulid W. Blasting Principles for Open Pit Mining. Rotterdam, Netherlands: AA Balkema; 1999.
- [5] Grady D, Kipp M. Geometric statistics and dynamic fragmentation. J Appl Phys. 1985;58:1210-22.
- [6] Udy LL, Lownds CM. The Partition of Energy in Blasting with non-ideal Explosives. Proceedings of the 3rd International Symposium on Rock Fragmentation by Blasting, Fragblast 3. Australia, Brisbane: CRC Press: Taylor and Francis Group; 1990. p. 37-43.
- [7] Wyllie DC, Mah C. Rock slope engineering: CRC Press; 2004.
- [8] Yang H-S, Rai P. Characterization of fragment size vis-à-vis delay timing in quarry blasts. Powder Technol. 2011;211:120-6.
- [9] Enayatollahi I, Bazzazi AA, Asadi A. Comparison between neural networks and multiple regression analysis to predict rock fragmentation in open-pit mines. Rock Mech Rock Eng. 2014;47:799-807.
- [10] Esmaeili M, Salimi A, Drebenstedt C, Abbaszadeh M, Bazzazi AA. Application of PCA, SVR, and ANFIS for modeling of rock

- fragmentation. *Arabian Journal of Geosciences*. 2014;1-13.
- [11] Ebrahimi E, Monjezi M, Khalesi MR, Armaghani DJ. Prediction and optimization of back-break and rock fragmentation using an artificial neural network and a bee colony algorithm. *B Eng Geol Environ*. 2015;1-10.
- [12] Shams S, Monjezi M, Majd VJ, Armaghani DJ. Application of fuzzy inference system for prediction of rock fragmentation induced by blasting. *Arabian Journal of Geosciences*. 2015;1-14.
- [13] Kuznetsov V. The mean diameter of the fragments formed by blasting rock. *J Min Sci*. 1973;9:144-8.
- [14] Cunningham C. The Kuz-Ram model for prediction of fragmentation from blasting. *Proceedings of the 1st International Symposium on Rock Fragmentation by Blasting, Fragblast 1*. Lulea Univ. Technol., Lulea, Sweden: CRC Press: Taylor and Francis Group; 1983. p. 439-53.
- [15] Bond FC. *Crushing and grinding calculations*: Allis-Chalmers Manufacturing Company; 1961.
- [16] Da-Gama C. Use of comminution theory to predict fragmentation of jointed rock masses subjected to blasting. *Proceedings of the 1st International Symposium on Rock Fragmentation by Blasting, Fragblast 1*. Lulea Univ. Technol., Lulea, Sweden: CRC Press: Taylor and Francis Group; 1983. p. 565-79.
- [17] Cunningham C. Fragmentation estimations and the Kuz-Ram model-Four years on. *Proceedings of the 2nd International Symposium on Rock Fragmentation by Blasting, Fragblast 2*. Keystone, Colorado: CRC Press: Taylor and Francis Group; 1987. p. 475-87.
- [18] Lilly PA. An empirical method of assessing rock mass blastability. *Large Open Pit Mining Conference*. Australia: The AusIMM/IE Aust Newman Combined Group; 1986.
- [19] Kou S, Rustan A. Computerized design and result prediction of bench blasting. *Proceedings of the 4th International Symposium on Rock Fragmentation by Blasting, Fragblast 4*. Vienna, Austria: CRC Press: Taylor and Francis Group; 1993. p. 5-8.
- [20] Kihlstrom B. The Swedish Wide Space Blasting Technique. *National Symposium on Rock Fragmentation Australian Geomechanics Society, Adelaide, Special Addresses and Discussion 1973*. p. 8-14.
- [21] Sanchidrian JA, Segarra P, Burden S, López LM. On the use of rock constants in bench blast design methods. *Proceedings of the 7th International Symposium on Rock Fragmentation by Blasting, Fragblast 7*. Beijing, China: CRC Press: Taylor and Francis Group; 2002. p. 396-405.
- [22] Persson P-A, Holmberg R, Lee J. *Rock blasting and explosives engineering*: CRC Press: Taylor and Francis Group; 1993.
- [23] Chung SH, Katsabanis P. Fragmentation prediction using improved engineering formulae. *Proceedings of the 6th International Symposium on Rock Fragmentation by Blasting, Fragblast 6*. Johannesburg, South Africa: CRC Press: Taylor and Francis Group; 2000. p. 198-207.
- [24] Ouchterlony F. The Case for the Median Fragment Size as a Better Fragment Size Descriptor than the Mean. *Rock Mech Rock Eng*. 2015;49:1-22.
- [25] Rosin P, Rammler E. The laws governing the fineness of powdered coal. *J Inst Fuel*. 1933;7:29-36.
- [26] Gilvarry J. Fracture of brittle solids. I. Distribution function for fragment size in single fracture (theoretical). *J Appl Phys*. 1961;32:391-9.
- [27] Gilvarry J, Bergstrom B. Fracture of brittle solids. II. Distribution function for fragment size in single fracture (experimental). *J Appl Phys*. 1961;32:400-10.
- [28] Cunningham C. Keynote address—optical fragmentation assessment, a technical challenge. *Proceedings of the 5th International Symposium on Rock Fragmentation by Blasting, Fragblast 5*. Montreal, Quebec, Canada: CRC Press: Taylor and Francis Group; 1996. p. 13-21.
- [29] Da-Gama C, Jimeno C. Rock fragmentation control for blasting cost optimization and environmental impact abatement. *Proceedings of the 4th International Symposium on Rock Fragmentation by Blasting, Fragblast 4*. Vienna, Austria: CRC Press: Taylor and Francis Group; 1993.
- [30] Lu P, Latham J-P. A model for the transition of block sizes during fragmentation blasting of rock masses. *Proceedings of the 6th International Symposium on Rock Fragmentation by Blasting, Fragblast 6*. Johannesburg, South Africa: CRC Press: Taylor and Francis Group; 1998. p. 341-68.
- [31] Kanchibotla SS, Valery W, Morrell S. Modelling fines in blast fragmentation and its impact on crushing and grinding. *Explo '99—A conference on rock breaking*. Kalgoorlie, Australia: The Australasian Institute of Mining and Metallurgy; 1999. p. 137-44.
- [32] Grundstrom C, Kanchibotla S, Jankovich A, Thornton D, Pacific DDNA. Blast fragmentation for maximising the sag mill throughput at Porgera Gold Mine. *Proceedings of the Annual Conference on Explosives and Blasting Technique: ISEE; 1999; 2001*. p. 383-400.
- [33] Svahn V. Generation of fines around a borehole: a laboratory study. *Proceedings of the 7th International Symposium on Rock Fragmentation by Blasting, Fragblast 7*. Beijing, China: CRC Press: Taylor and Francis Group; 2002. p. 122-7.
- [34] Svahn V. *Generation of fines in bench blasting*. 2003.
- [35] Moser P. Less fines production in aggregate and industrial minerals industry. *Proceedings of the Annual Conference on Explosives and Blasting Technique: ISEE; 1999; 2004*. p. 109-22.
- [36] Hall J, Brunton I. Critical comparison of Julius Kruttschnitt Mineral Research Centre (JKMRC) blast fragmentation models. *Explo 2001: AusIMM; 2001*. p. 207-12.
- [37] Ouchterlony F. The Swebrec[®] function, linking fragmentation by blasting and crushing. *Min Tech (Trans Inst Min Metal A)*. 2005;114:A29–A44.
- [38] Spathis A. A correction relating to the analysis of the original Kuz-Ram model. *Proceedings of the 8th International Symposium on Rock Fragmentation by Blasting, Fragblast 8*. Santiago, Chile: CRC Press: Taylor and Francis Group; 2004. p. 201-5.
- [39] Sanchidrián JA, Ouchterlony F, Segarra P, Moser P. Size distribution functions for rock fragments. *Int J Rock Mech Min Sci*. 2014;71:381-94.
- [40] Carlsson O, Nyberg L. A method for estimation of fragmentation size distribution with automatic image processing. *Proceedings of the 1st International Symposium on Rock Fragmentation by Blasting, Fragblast 1*. Lulea Univ. Technol., Lulea, Sweden: CRC Press: Taylor and Francis Group; 1983. p. 333-45.
- [41] Kemeny JM. Practical technique for determining the size distribution of blasted benches, waste dumps and heap leach sites. *Int J Rock Mech Min Sci and Geomech Abs*. 1995;4:170A.
- [42] Kemeny J, Girdner K, Bobo T, Norton B. Improvements for fragmentation measurement by digital imaging: accurate estimation of fines. *Proceedings of the 6th International Symposium on Rock Fragmentation by Blasting, Fragblast 6*. Johannesburg, South Africa: CRC Press: Taylor and Francis Group; 1999. p. 103-10.

- [43] Kemeny J, Mofya E, Kaunda R, Lever P. Improvements in blast fragmentation models using digital image processing. Proceedings of the 7th International Symposium on Rock Fragmentation by Blasting, Fragblast 7. Beijing, China: CRC Press: Taylor and Francies Group; 2002. p. 311-20.
- [44] Latham J-P, Kemeny J, Maerz N, Noy M, Schleifer J, Tose S. A blind comparison between results of four image analysis systems using a photo-library of piles of sieved fragments. Proceedings of the 8th International Symposium on Rock Fragmentation by Blasting, Fragblast 8. Santiago, Chile: CRC Press: Taylor and Francies Group; 2003. p. 105-32.
- [45] Sudhakar J, Adhikari G, Gupta R. Comparison of fragmentation measurements by photographic and image analysis techniques. *Rock Mech Rock Eng.* 2006;39:159-68.
- [46] Blair D. Curve-fitting schemes for fragmentation data. Proceedings of the 8th International Symposium on Rock Fragmentation by Blasting, Fragblast 8. Santiago, Chile: CRC Press: Taylor and Francies Group; 2004. p. 137-50.